Energy 201 (2020) 117512

Contents lists available at ScienceDirect

Energy

journal homepage: www.elsevier.com/locate/energy

Economic dispatch analysis of regional Electricity–Gas system integrated with distributed gas injection

Gui-Xiong He [a, b, **], Hua-guang Yan [b], Lei Chen [a], Wen-Quan Tao [a, *]

[a] Key Laboratory of Thermo-Fluid Science and Engineering, Ministry of Education, Xi'an Jiaotong University, Xi'an, 710049, China
[b] State Key Laboratory of Security and Energy Saving. China Electric Power Research Institute, Beijing, 100192, China

ARTICLE INFO

Article history:
Received 11 August 2019
Received in revised form
26 March 2020
Accepted 28 March 2020
Available online 13 April 2020

Keywords:
Regional electricity–gas system
Economic dispatch
Distributed gas injection
Multienergy flow

ABSTRACT

With the development of energy conversion technologies such as combined heat and power and gas power generation, various forms of energy, such as the electricity, gas, and heat of regional integrated energy systems have become highly coupled. Aiming at regional electricity–gas systems (REGS), this paper focuses on the interaction between an electricity power system and a natural gas system. A comprehensive analytical model of the REGS combined with distributed gas injection is proposed, where a regional energy station (RES) is considered as an energy coupling link. The REGS's energy flow is optimized to minimize the operation cost of the RES by comprehensively considering the cost of distributed gas injection, the penalty of wind curtailment, and the constraints of the energy network. Furthermore, multiple RESs and distributed gas injections are used as a control to study the effects of various adjustable resources on the economics of REGS' operating costs, flexibility of renewable energy consumption, and safety of pressure support capabilities. Subsequently, a system optimization scheduling strategy without considering gas injection point and the corresponding strategy considering hydrogen or upgraded biogas as gas injection temperament are studied. Numerical example shows that with the introduction of distributed gas injection points, the economic dispatch strategy considering the upgrade of biogas and hydrogen injection improved the economic, pressure reduction level, and wind power consumption rate of the system, which are important for improving the stability and flexibility of REGSs.

1. Introduction

Energy is the basis of national development. With the efficiency improvement of industrial production and the continuous improvement of living standards of residents, energy demand has increased significantly. This resulted in an increasingly serious contradiction between energy development and environmental issues. Therefore, energy issues have become a popular topic in academia and industry in recent years. The use of traditional fossil fuels, such as coal and petroleum, is not sustainable and inefficient as it causes serious environmental pollution. Therefore, improving the efficiency of energy utilization and developing large-scale renewable energy resources are necessitated to resolving these conflicts. The existing models of individual energy supply systems, which must be individually planned, individually designed, and operated independently must be modified, and a unified integrated energy system should be constructed.

An integrated energy system (IES) refers to an energy generation–supply–consumption integration system formed from the organic coordination and optimization of energy production, transmission, distribution, conversion, storage, and consumption during planning, construction, and operation [1]. An IES includes an electricity power system (EPS), a natural gas system (NGS), a thermal power system, and other coupling components. With scientific dispatch among various subsystems, an IES can achieve efficient energy use, satisfy users' multienergy cascade utilization and ensure a safe and reliable social energy supply. IESs can be categorized into regional integrated energy systems (RIESs) and user-level IESs based on geographic factors, energy generation, transmission, distribution, and use characteristics [2]. Different energy conversion, distribution, and utilization scenarios can be observed in different RIESs. This paper focuses on the coupling

* Corresponding author.
** Corresponding author.
E-mail addresses: 2464799833@qq.com (G.-X. He), hgyan@epri.sgcc.com.cn (H.-g. Yan), chenlei@mail.xjtu.edu.cn (L. Chen), wqtao@mail.xjtu.edu.cn (W.-Q. Tao).

https://doi.org/10.1016/j.energy.2020.117512
0360-5442/

Nomenclature

Abbreviations	*Description*
RIES	Regional integrated energy system
REGS	Regional electricity–gas system
RES	Regional energy station
EPS	Electricity power system
NGS	Natural gas system
IES	Integrated energy system
PSO	Particle swarm optimization
PEC	Power electronics converter
CHP	Combined heat and power
GB	Gas boilers
CAC	Central air conditioning
P2G	Power to gas
GCV	Gross caloric valve
OpenDSS	Open distribution system simulator
SG	Specific gravity

between an EPS and NGS with an RIES as the background.

Because traditional energy systems are individually designed and planned separately, the interaction between different energy systems and multienergy complementarities are ignored in the traditional systems [3]. The regional energy station (RES) model and the coupling coordination between NGSs and EPSs are introduced herein. An RES is a core component of a power–natural-gas coupling link, which can be regarded as a multienergy coordinated operation center in regional electricity–gas systems (REGSs) [4]. The characteristics of energy flow conversion and distribution by the RES model are analyzed herein.

A brief review of the coupling between an EPS and NGS in the existing literature is provided as follows. In Ref. [5], an interconnection model and optimization framework of an electricity–gas system were constructed, and the steady-state analytical method of an EPS was used in NGS analysis. Based on a similar analysis method, Geidl and Andersson [6] introduced the integration model and unified scheduling of an IES based on an energy hub model. Shahidehpour et al. [7] discussed the impact of natural gas equipment and price on EPS scheduling and analyzed the coupling relationship between an EPS and NGS at the price level. Abeysekera [8] discussed the different components of an NGS and the conditions of gas injection. Trifonov [9] indicated that surplus energy from renewable energy systems can be stored and subsequently used to support electrical natural gas grids. The abovementioned studies primarily focused on cross-regional IESs, whereas discussions on RIESs and there changes to the state of NGSs were few. For example, system changes caused by gas injection points were not considered. Owing to economic dispatch and other reasons, the load regulation of NGS will cause changes in the state of a natural gas network. With the coordination of different types of RESs and the adjustment of temperament and flow rate of gas injection, the operating cost of RESs can be reduced effectively, and the rate of renewable energy consumption will increase, which have not been discussed in previous studies.

This paper is organized as follows: Section 2 presents a comprehensive model of multienergy flow in REGSs, which includes an EPS model, NGS model, and RES model. Section 3, an REGS economic dispatch model that minimizes the operation cost of RESs considering gas injection and wind curtailment costs is described. Furthermore, the method and framework for solving the REGS economic dispatch model using particle swarm optimization (PSO) are proposed. Section 4 introduces a typical REGS case and discusses the effect of hydrogen or upgraded biogas injection points on the economics and wind power consumption rate of the system. Finally, conclusions and recommendations are presented in Section 5.

2. Comprehensive model of multienergy flow in REGS

The RIES described herein exhibits complex energy coupling. It comprises a distributed terminal integrated energy unit system and a coupled centralized energy supply network. The region considered in this study is either a city or local township. Furthermore, considering the basic status of electricity and gas in a terminal energy system, this article focuses on these two types of energies. For RIESs, this article focuses on the method of building a steady-state model. The law of mass conservation and Kirchhoff's law were adhered to during the construction of the model [10]. The steady-state model of the REGS is expressed as follows:

$$\begin{cases} f_E(x_e, x_g, x_{res}) = 0 \\ f_{NG}(x_e, x_g, x_{res}) = 0 \\ f_{RES}(x_e, x_g, x_{res}) = 0 \end{cases}. \tag{1}$$

The three equations above represent the energy flow equations of the EPS, NGS, and RES in the REGS, which represent the energy constraints that must be satisfied by the REGS in a steady-state operation. x_e represents EPS variables, such as line power, node phase angle, and node voltage amplitude;x_g represents NGS variables, such as node pressure and pipeline flow; x_{res}represents energy coupling factors such as power conversion coefficients. Owing to the components such as gas turbines and RESs, the steady-state operation of a single energy system is affected by other energy systems. Therefore, the three equations above include EPS, NGS, and energy coupling link variables. Next, we will focus on the construction and solution of the equations above.

2.1. EPS steady-state model

The power link in an REGS is primarily the distribution network. The main features of such network include the following: radial operation, large ratio of resistance to reactance of tributaries, unbalanced three-phase, multiple branches, and access to renewable energy. Moreover, with the increasingly close coupling of multiple energy sources in an IES, an EPS is not only the output target of other energy sources, but also the energy supplier of coupling energy in other energy systems. The basis of power flow calculation is node power balance equations, which are presented as follows [11]:

$$\begin{cases} P_i^p = V_i^p \sum_{k=1}^{N} \sum_{m\in(a,b,c)} V_k^m \left(G_{ik}^{pm} \cos\theta_{ik}^{pm} + B_{ik}^{pm} \sin\theta_{ik}^{pm} \right) \\ Q_i^p = V_i^p \sum_{k=1}^{N} \sum_{m\in(a,b,c)} V_k^m \left(G_{ik}^{pm} \sin\theta_{ik}^{pm} - B_{ik}^{pm} \cos\theta_{ik}^{pm} \right) \end{cases}, \tag{2}$$

where $P_i^p$and Q_i^p are the active and reactive net loads of node i and phase p, respectively; N is the number of nodes; $\theta_{ik}^{pm}$is the p- and m-phase angle differences between i and node k, respectively; G and B are the conductance and susceptance, respectively. Because the power flow solving method is well known, it was directly applied in this study and its details are omitted herein.

2.2. NGS model and gas injection model

2.2.1. NGS model

The NGS primarily includes two parts [12]: nodes and branches. The NGS primarily comprises types of nodes: (i) a pressure known node, which is generally a gas source point with a known pressure. The flow passing through this point is the quantity to be calculated. It is similar to the balanced node in an EPS; (ii) a flow-known node, which is generally a load node, and its pressure is a demand amount, which is similar to a PQ node in an EPS. When the pressure and flow of the load node are known, they can be compared with PV nodes in an EPS. The branches of an NGS can be categorized into two types: branches with and without a compressor. For branches in NGSs, the pipeline flow is related to the pressure at both ends of the pipeline. The formula to calculate pipeline flow is related to the pressure level and the corresponding network parameters. In this study, we primarily investigate low-pressure systems, whose pressure range is 0–75 mbar [12]. A pipeline flow can be modeled as follows [13,14]:

$$\begin{cases} Q_{pipe} = 5.72 \times 10^{-4} \sqrt{\dfrac{(p_1 - p_2)D^5}{fSL}} \\ f = 0.0044\left(1 + \dfrac{12}{0.276D}\right) \end{cases}, \tag{3}$$

where $Q_{pipe}$is the pipe volume flow in standard pressure temperature; $p_1$is the pressure at the pipe's starting node; $p_2$is the pressure at the pipe end node; D is the diameter of the pipeline; f is the friction factor; S is the specific gravity; L is the pipeline length.

For each node of the NGS, the law of flow conservation should be satisfied. The model of the node is shown in the following formula [8]:

$$A_{NGS}\eta + \upsilon = 0, \tag{4}$$

where $A_{NGS}$is the incidence matrix of the nodes and pipelines in the NGS; $\eta$is the natural gas pipeline flow vector in the NGS; $\upsilon$is the node payload vector in the NGS.

2.2.2. NGS energy flow calculation

The energy flow calculation of an NGS is similar to that of an EPS. Similarly, based on the law of mass conservation and Kirchhoff's law, natural gas power flow solutions focusing on nodes and closed loops can be formed; furthermore, high-order iterative algorithms can be used to solve high-dimensional nonlinear equations [15]. In this study, the node-method power flow equation was used. For an n-node NGS, according to Equation (1), when using the Newton–Raphson method to solve the steady-state flow of NGSs, the correction equations of the node pressure at the k-th iteration are as follows [12]:

$$\begin{cases} F\left(x_g^{(k)}\right) = J^{(k)}\Delta x_g^{(k)} \\ x_g^{(k+1)} = x_g^{(k)} - \Delta x_g^{(k)} \end{cases} \tag{5}$$

$$F\left(x_g^{(k)}\right) = \begin{bmatrix} F_{NG1}\left[x_{g1}^{(k)}, x_{g2}^{(k)}, \cdots, x_{gn}^{(k)}\right] \\ F_{NG2}\left[x_{g1}^{(k)}, x_{g2}^{(k)}, \cdots, x_{gn}^{(k)}\right] \\ \vdots \\ F_{NGn}\left[x_{g1}^{(k)}, x_{g2}^{(k)}, \cdots, x_{gn}^{(k)}\right] \end{bmatrix}, \tag{6}$$

where Equation (6) is the error vector of the function sought; $J^{(k)}$ is the Jacobian matrix; $\Delta x_g^{(k)}$is the correction vector. With iterations, the required variables gradually approach the true solution of the system until the convergence conditions are satisfied.

2.2.3. Gas injection model of NGS

The gas compositions in NGSs differ, and changes in the gas composition may affect the temperament and hence the pressure in the pipeline. Therefore, when injecting gas into the network, the effect of different gas compositions on the state of the network must be considered. The energy demand at a node depends on the gas device connected to a specific location in the network. In conventional gas network analysis, gas flow demand is set as equal to the energy demand of a node. It is appropriate for the network when the gas composition throughout the network is uniform and the gas flow demand is proportional to the combustion energy demand [13], which can be written as follows:

$$E_{load} \propto G_{load}, \tag{7}$$

where E_{load}represents the energy demand; G_{load}represents the gas flow rate demand.

The required combustion energy for gas node i can be calculated as follows:

$$E_{load,i} = G_{load,i} \times GCV_i, \tag{8}$$

where $GCV_i$is the gross calorific value of gas.

In areas with multiple sources of supply, the composition of the gas mixture throughout the network may vary. A distributed gas supply is modeled as a gas flow injection at a specific node. The gas flow injected at gas node i can be calculated as follows [13]:

$$G_{source,i} = -\frac{E_{source,i}}{GCV_{source,i}}, \tag{9}$$

where $G_{source,i}$is gas flow rate injected; $E_{source,i}$is the gaseous energy injection rate.

For natural gas nodes with both demand and distributed injection, the net gas load of gas node i according to Equations (8) and

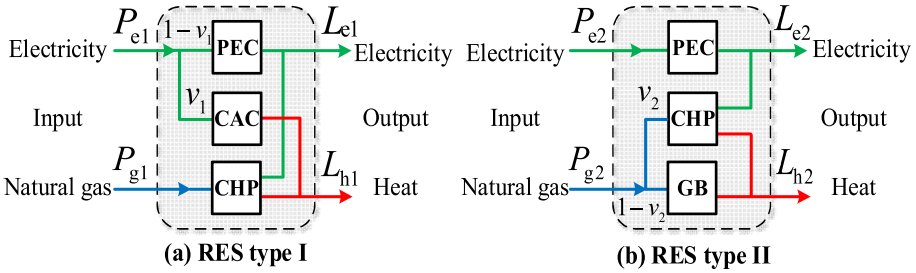

Fig. 1. Regional energy station (RES) model.

(9) can be written as follows:

$$\begin{cases} E_{net\ \ demand,i} = E_{load,i} - E_{\mathrm{supply},i} \\ G_{net\ \ demand,i}\left(\dfrac{m^3}{s}\right) = \dfrac{E_{load,i} - E_{source,i}\left(\dfrac{kJ}{s}\right)}{GCV_{node}\left(\dfrac{kJ}{m^3}\right)} \end{cases}. \tag{10}$$

A gas injection point typically appears in a low-pressure NGS. Unlike an EPS distributed generation, which is directly connected to an EPS, a small-diameter gas distribution pipeline must be installed for the gas injection point. This means that the local network structure of the NGS will change. Furthermore, the corresponding node–branch matrix and the NGS flow calculation matrix will have an additional dimension. Using the error equation as an example, the dimension-added equation is set as follows, where formulas enclosed in red brackets are dimensions added to the corresponding matrix:

$$\begin{bmatrix} F_{\mathrm{NG1}}\left[x_{\mathrm{g1}}^{(k)},x_{\mathrm{g1}}^{(k)},\ldots,x_{\mathrm{g\_add}}^{(k)}\right] \\ F_{\mathrm{NG2}}\left[x_{\mathrm{g1}}^{(k)},x_{\mathrm{g1}}^{(k)},\ldots,x_{\mathrm{g\_add}}^{(k)}\right] \\ \cdots \\ \left\{F_{\mathrm{NG\_add}}\left[x_{\mathrm{g1}}^{(k)},x_{\mathrm{g1}}^{(k)},\ldots,x_{\mathrm{g\_add}}^{(k)}\right]\right\} \end{bmatrix} = \begin{bmatrix} \dfrac{\partial F_{\mathrm{NG1}}}{\partial P_1} & \cdots & \overbrace{\dfrac{\partial F_{\mathrm{NG1}}}{\partial P_{\mathrm{N\_add}}}} \\ \cdots & \cdots & \cdots \\ \left\{\dfrac{\partial F_{\mathrm{NG\_add}}}{\partial P_1}\right. & \cdots & \underbrace{\left.\dfrac{\partial F_{\mathrm{NG\_add}}}{\partial P_{\mathrm{N\_add}}}\right\}} \end{bmatrix}$$

$$\times \begin{bmatrix} \Delta x_{\mathrm{g1}}^{(k)} \\ \cdots \\ \left\{\Delta x_{\mathrm{g\_add}}^{(k)}\right\} \end{bmatrix} = \begin{bmatrix} a_{11} & \cdots & \overbrace{a_{1,\mathrm{add}}} \\ \cdots & \cdots & \cdots \\ \{a_{\mathrm{add},1} & \cdots & \underbrace{a_{\mathrm{add,add}}\}} \end{bmatrix} \begin{bmatrix} Q_{\mathrm{g1}}^{(k)} \\ \cdots \\ \left\{Q_{\mathrm{g\_add}}^{(k)}\right\} \end{bmatrix}$$

$$- \begin{bmatrix} L_{\mathrm{g1}} \\ \cdots \\ \left\{L_{\mathrm{g\_add}}\right\} \end{bmatrix} \tag{11}$$

Here, $a$is the element of the node association matrix; $L_g$is the node load.

2.3. RES model

Traditional energy storage is limited by factors such as geographical environment, physical conditions, and economic conditions. For such an energy storage, the analysis of system operating characteristics with complex coupling relationships is limited in some aspects. Therefore, large-scale energy storage with mature technology and cost-effective network levels are important.

In this context, a RES is considered. Based on the mathematical model of an energy hub, an RES uses power electronics converters (PECs), combined heat and power (CHP), gas boilers (GBs), central air-conditioning (CAC), and other components to achieve optimal energy dispatch through energy conversion and distribution, which are conducive to the future construction of the RIES basic framework with diverse energy types and complex coupling characteristics. The model of a RES is shown in Fig. 1.

The input and output of energy are connected through the energy coupling matrix. By changing the RES distribution coefficient, energy will be exchanged and distributed, thereby enabling a power interaction between the RES and RIES [16]. For the modeling of power–natural-gas coupling, two typical methods are presented herein.

The first type can be expressed as a constraint equation as follows [17]:

$$\begin{bmatrix} L_{e1} \\ L_{h1} \end{bmatrix} = \begin{bmatrix} 1-\upsilon_1 & \eta^{CHP\_ge} \\ \upsilon_1\eta^{CAC} & \eta^{CHP\_gh} \end{bmatrix} \begin{bmatrix} P_{e1} \\ P_{g1} \end{bmatrix} \tag{12}$$

Meanwhile, the second type can be expressed as a constraint equation as follows [17]:

$$\begin{bmatrix} L_{e2} \\ L_{h2} \end{bmatrix} = \begin{bmatrix} \eta^{T} & \upsilon_2\eta^{CHP\_ge} \\ 0 & (1-\upsilon_2)\eta^{GB} + \upsilon_2\eta^{CHP\_gh} \end{bmatrix} \begin{bmatrix} P_{e2} \\ P_{g2} \end{bmatrix}, \tag{13}$$

where L represents the vector of the energy demand; P represents the vector of the energy supply; $\upsilon_1$and $\upsilon_2$represent the dispatch factor of RES types I and II, respectively;η^{CHP_ge} and η^{CHP_gh}represent the gas–electricity and gas–heat-energy conversion efficiencies in the CHP, respectively;η^{T}, **and** η^{GB}represent the energy conversion efficiency of the power transformer, CAC, and GB, respectively.

3. Hierarchical optimization of REGS

A RES serves as a coordinator in each energy conversion process and contributes to the economic operation of the system [18–22]. By adjusting the distribution coefficient, the user's load is supplied by different equipment to achieve an economically optimized operation. For example, when the electricity price is high and the gas price is low, a CHP is primarily used to supply power, which can reduce operating costs. However, owing to the uncertainty of renewable energy and the complex interaction between different energy systems, the economic dispatch of IEGSs remain challenging [[23]]. A method to achieve various objectives and manage an entire system by layering an REGS is presented in this section [[24]]. To optimize and schedule REGSs, the optimization objectives and operational constraints of four scenarios are primarily considered. In this study, an RES is regarded as an integrated energy service provider, and the optimization objective is the lowest comprehensive cost of RESs while considering the cost of purchasing gas at the distributed gas injection point. In addition, the consumption of renewable energy is considered, and wind curtailment is added to the objective function as a penalty term.

3.1. Objectives

3.1.1. Case 1: economic dispatch of RES decoupling energy system

In Case 1, the EPS and NGS are in a decoupled state, whereas power and the natural gas load are supplied through transformers and gas boilers, respectively. The target function was set as follows:

$$\min C_{\mathrm{cost}} = \sum_{t=1}^{24}\left[\pi_{\mathrm{e},t}P_{\mathrm{e},t} + \pi_{\mathrm{g},t}P_{\mathrm{g},t} + \sum_{i=1}^{2}\lambda\left(P_{\mathrm{i},t}^{fw} - P_{\mathrm{i},t}^{w}\right)\right], \tag{14}$$

where $C_{\cos\ t}$is the total cost of the RES for purchasing electricity and natural gas; $\pi_{\mathrm{e},t}$is the electricity price at time t; $\pi_{\mathrm{g},t}$is the natural gas price at time t; $P_{\mathrm{e},t}$is the sum of the purchased power of the decoupled nodes at time t; $P_{g,t}$is the sum of the natural gas power of the decoupled nodes at time t; $\lambda$is the penalty coefficient of abandoned wind power; $P_{\mathrm{i},t}^{fw}$ and $P_{\mathrm{i},t}^{w}$are the maximum power generation and actual power generation of the i-th wind turbine in the t-th period, respectively.

3.1.2. Case 2: economic dispatch of RES coupled energy system

Case 2 utilizes the complementary and mutual benefit characteristics of different energies to optimize the multienergy flow of REGSs by adjusting RESs, thereby achieving economic optimization.

This paper focuses on the daily ahead economic dispatch of RESs, and the optimization target is the lowest comprehensive cost of RESs. The target function is set as follows:

$$\min C_{\text{cost}} = \sum_{t=1}^{24}\left[\frac{\pi_{\text{e-buy},t}+\pi_{\text{e-sell},t}}{2}P_{\text{e},t}+\frac{\pi_{\text{e-buy},t}-\pi_{\text{e-sell},t}}{2}|P_{\text{e},t}| + \pi_{\text{g},t}P_{\text{g},t}+\sum_{i=1}^{2}\lambda\left(P_{\text{i},t}^{fw}-P_{\text{i},t}^{w}\right),\right. \tag{15}$$

where $\pi_{\text{e-buy},t}$ is the purchase price of electricity at time t; $\pi_{\text{e-sell},t}$ is the price of a BEH to an EPS selling electricity at time t; $\pi_{\text{g},t}$ is the natural gas price at time t; $P_{\text{e},t}$ is the electric power consumed when the RES interacts with the EPS at time t; $P_{\text{g},t}$ is the natural gas power absorbed by the RES at time t; $P_{\text{i},t}^{fw}$ and $P_{\text{i},t}^{w}$ are the maximum and actual power generation of the i-th wind turbine in the t-th period, respectively.

3.1.3. Case 3: RES economic dispatch considering gas injection point of upgraded biogas

Case 3 considers the temperament of the injected gas as upgraded biogas. Similar to Case 2, the operation constraints of Case 3 contain equality constraints of the REGS and the corresponding inequality constraints. In addition, the upper and lower limits of the gas injection point flow must be supplemented. The optimization target of Case 3 is set as follows:

$$\min C_{\text{cost}} = \sum_{t=1}^{24}\left[\frac{\pi_{\text{e-buy},t}+\pi_{\text{e-sell},t}}{2}P_{\text{e},t}+\frac{\pi_{\text{e-buy}t}-\pi_{\text{e-sell},t}}{2}|P_{\text{e},t}| + \pi_{\text{bi}}P_{\text{inj},t}+\pi_{\text{g},t}P_{\text{g},t}+\sum_{i=1}^{2}\lambda\left(P_{\text{i},t}^{fw}-P_{\text{i},t}^{w}\right),\right. \tag{16}$$

where π_{bi} is the price of the upgraded biogas; $P_{\text{inj},\,t}$ is the natural gas power injected to the NGS in the t-th period.

3.1.4. Case 4: RES economic dispatch considering gas injection point of hydrogen

In Case 4, hydrogen was considered as the temperament of the injected gas. The natural-gas-pressure-load sensitivity relationship was analyzed. The corresponding operation constraints of Case 4 were the same as those of Case 3 and the optimization target of Case 4, which was set as follows:

$$\min C_{\text{cost}} = \sum_{t=1}^{24}\left[\frac{\pi_{\text{e-buy},t}+\pi_{\text{e-sell},t}}{2}P_{\text{e},t}+\frac{\pi_{\text{e-buy}t}-\pi_{\text{e-sell},t}}{2}|P_{\text{e},t}| + \pi_{\text{hy}}P_{\text{inj},t}+\pi_{\text{g},t}P_{\text{g},t}+\sum_{i=1}^{2}\lambda\left(P_{\text{i},t}^{fw}-P_{\text{i},t}^{w}\right),\right. \tag{17}$$

where π_{hy} is the price of hydrogen; $P_{\text{inj},\,t}$ is the natural gas power injected to the NGS in the t-th period.

3.2. Constraints

3.2.1. EPS constraints

The three-phase EPS constraints are as follows:

$$f_e(P,Q,V,\theta)=0 \tag{18}$$

$$\begin{cases} V_{\min}\le V_i^a\le V_{\max} \\ V_{\min}\le V_i^b\le V_{\max} \\ V_{\min}\le V_i^c\le V_{\max} \end{cases} \tag{19}$$

$$P_{\text{WT\_min}}\le P_{WT}\le P_{\text{WT\_max}}, \tag{20}$$

where P and Q represent the active power and reactive power of the EPS, respectively; V and θrepresent the node voltage and phase angle of the EPS, respectively; V_i^a, V_i^b *and* V_i^crepresent the three-phase voltages at bus i;$V_{\min}$and $V_{\max}$represent the lower and upper bounds of the bus voltage, respectively; P_{WT} represents the wind turbine output in the RES; $P_{\text{WT_min}}$and $P_{\text{WT\_max}}$ represent the lower and the upper bounds of the wind turbine output in the RES, respectively.

3.2.2. NGS constraints

$$f_g(F,n,r)=0 \tag{21}$$

$$n_{\min}\le n_i\le n_{\max} \tag{22}$$

$$r_{\min}\le r\le r_{\max} \tag{23}$$

$$I_{\min}\le I\le I_{\max}, \tag{24}$$

where F represents the gas flow; n is the gas flow supplied by the gas wells; $n_{\min}$and $n_{\max}$represent the lower and upper bounds of the gas flow, respectively; r is the gas load; $r_{\min}$and $r_{\max}$represent the lower and upper bounds of the gas load, respectively; I represents the volume of hydrogen or upgraded biogas injected into the gas injection point; $I_{\min}$and $I_{\max}$represent the lower and upper bounds of the volume of the hydrogen or upgraded biogas, respectively.

3.2.3. RES constraints

The equality constraints of the RES are given in Equations (12) and (13), and the inequality constraints of the RES are as follows:

$$P_{PEC\_\min}\le P_{PEC}\le P_{PEC\_\max} \tag{25}$$

$$P_{\text{CAC\_min}}\le P_{CAC}\le P_{\text{CAC\_max}} \tag{26}$$

$$P_{\text{CHP\_min}}\le P_{CHP}\le P_{\text{CHP\_max}} \tag{27}$$

$$P_{\text{GB\_min}}\le P_{GB}\le P_{\text{GB\_max}}, \tag{28}$$

where P_{PEC}represents the PEC output in the RES; $P_{PEC_\min}$and $P_{PEC_\max}$represent the lower and upper bounds of the PEC output in RES, respectively; P_{CAC}represents the CAC output in the RES; P_{CHP}represents the CHP output in the RES; $P_{\text{CHP_min}}$and $P_{\text{CHP_max}}$represent the lower and upper bounds of the CHP output in RES, respectively; P_{GB}represents the GB output in the RES; $P_{\text{GB_min}}$and $P_{\text{GB_max}}$represent the lower and upper bounds of the GB output in the RES, respectively.

3.3. NGS network state analysis and steady solution of REGS

The transmission of energy between NGSs will result in changes in the temperament. Furthermore, with the application of power to gas (P2G) technology [18], the connection between an NGS and EPS become narrower. The hydrogen obtained by P2G technology can

be sent to the required industrial sector as a fuel or injected into an NGS at a certain proportion. Furthermore, methanation technology can produce an upgraded methane to be injected it into an NGS [19]. These gases are often injected into an NGS in the form of distributed gas injection, which results in changes in temperament and network structure of the NGS. The change in NGS structure significantly affects NGSs and RIESs. This paper will focus on this issue.

3.3.1. Effect of different temperaments on NGS

An NGS can withstand changes in its temperament within a certain range, and this change will affect its nodal pressure and pipeline flow. In a steady-state calculation, with certain assumptions [20] combined with Darcy's equation [13], the pressure drop d_p of a natural gas along a pipeline can be expressed as follows:

$$\begin{cases} d_p = -0.5 \times \dfrac{\rho v^2 \lambda \times d_x}{D} \\ \mathrm{Re} = \dfrac{\rho v D}{\eta} \end{cases}, \tag{29}$$

where $d_x$is the pipeline length; D is the inner diameter of the pipeline; $\rho$is the mass density of the natural gas under the pressure and temperature conditions of the pipeline; v is the natural gas flow rate; $\lambda$is the friction coefficient that is related to the pipeline roughness and the Reynolds number of the fluid Re; $\eta$is the dynamic viscosity of the gas mixture at the pressure and temperature of the pipeline.

Furthermore, the temperament of natural gas affects its gross calorific value, which is the amount of heat released when a unit mass of natural gas is completely burned, as described by a gross caloric valve (GCV). The energies released by natural gases of different temperaments under the same conditions differ. A change in the NGS network state will affect the variables above and hence the pressure drop.

3.3.2. Sensitivity analysis for NGS

In an REGS, load changes in an NGS can significantly affect the network states. The sensitivity analysis method was used in this study to investigate the effects of such changes. A sensitivity analysis can provide information regarding changes in the node pressure with changing loads. The node-pressure–load-sensitivity matrix can assist in obtaining the optimization position of the NGS load regulation.

In Equation (1), the NGS equation can be set as$f(p, l) = 0$, in which p is the node pressure and l is the node load. Let the steady-state operating point of the NGS be(p_0, l_0), which will change into $(p_0 + \Delta p, l_0 + \Delta l)$under disturbance. The relationship between p and l can be obtained by a Taylor series expansion for$f(p, l) = 0$ at point (p_0, l_0), ignoring the high-order terms. It is set as follows:

$$\Delta p = -\left(\frac{\partial f}{\partial p}\right)^{-1} \frac{\partial f}{\partial l} \Delta l \tag{30}$$

Therefore, the node-pressure–load-sensitivity matrix of NGS S can be described as follows:

$$S = -\left(\frac{\partial f}{\partial p}\right)^{-1} \frac{\partial f}{\partial l} \tag{31}$$

Because the value of variation l is definite and known, $\partial f / \partial l$ is$diag[1 \ldots 1]$. Subsequently, S can be set as follows:

$$S = -\left(\frac{\partial f}{\partial p}\right)^{-1} \tag{32}$$

Equation (32) implies that the node-pressure–load-sensitivity matrix of the NGS is equal to the negative inversion of the Jacobian matrix of the NGS load flow solution.

3.3.3. Comprehensive solution to steady-state problems of REGS

The steady-state solution of an RIES is based on Matlab and the open-distribution system simulator (OpenDSS) platform. A brief introduction to OpenDSS is as follows. Because the traditional balance-analysis-based power flow analysis tool cannot satisfy the requirements of the IES for power flow calculation, the three-phase power flow analysis tool in OpenDSS was used in this study to solve an EPS power flow. Developed by the EPRI, OpenDSS provides models for renewable energy generation equipment and power storage devices, enabling the three-phase unbalanced modeling of EPSs (loads and lines) and the rapid simulation of distributed power supplies [21].

The optimal economic scheduling model in this study considers various schedulable resources, including energy links (such as cogeneration units) that can be easily controlled, as well as intermittent and random energy links (such as new energy generation). Therefore, the model presents complex high-dimensional, nonconvex, and nonlinear hybrid characteristics. It is difficult to obtain a satisfactory solution by the conventional solution method. PSO is a global random search algorithm based on swarm intelligence, which has been widely used in solving nonlinear problems in recent years. In this study, PSO was used to analyze the steady-state currents of an REGS. The solution was primarily categorized into three parts, and the corresponding flow chart is shown in Fig. 2. The solution procedure includes five steps as follows:

1) First, initialize the system and input information such as load and renewable energy;
2) Solve the NGS energy flow. If a gas injection point exists, then the number of correlation matrix dimensions, such as the node–branch incidence matrix must be updated; if a gas injection point does not exist, the pipeline flow and pressure are calculated iteratively by the Newton–Raphson method until the required accuracy is attained;
3) Further integrate the information through the RES and feed the result back to the EPS to solve the EPS energy flow;
4) Calculate the fitness value of each particle. Update the optimal position of the current population and the optimal position of all particles.
5) Determine whether the optimal position satisfies the requirement or whether the number of iterations has reached the maximum. If the condition is satisfied, end the calculation and output the result; otherwise, return to step (2) until the calculation result satisfies the converged condition.

4. Case studies

4.1. Case setting

In this study, a typical REGS was selected. Its system structure is shown in Fig. 3, which primarily includes the modified Institute of Electrical and Electronics Engineers 37-node EPS, an 11-node low-pressure NGS, and types I and II RESs. Among them, nodes 735 and 729 were connected with wind turbines whose rated powers were both 120 kW. The data source was provided by the China Electric Power Research Institute. Node 1 of the NGS was the gas source point, and Node 12 was the gas injection point. Hydrogen or upgraded biogas was considered as the temperament of the injected gas. The electric and thermal load demand of the RES are shown in Fig. 4(a) and (b), respectively. The energy prices of electricity, natural gas, hydrogen, and upgraded biogas are shown in

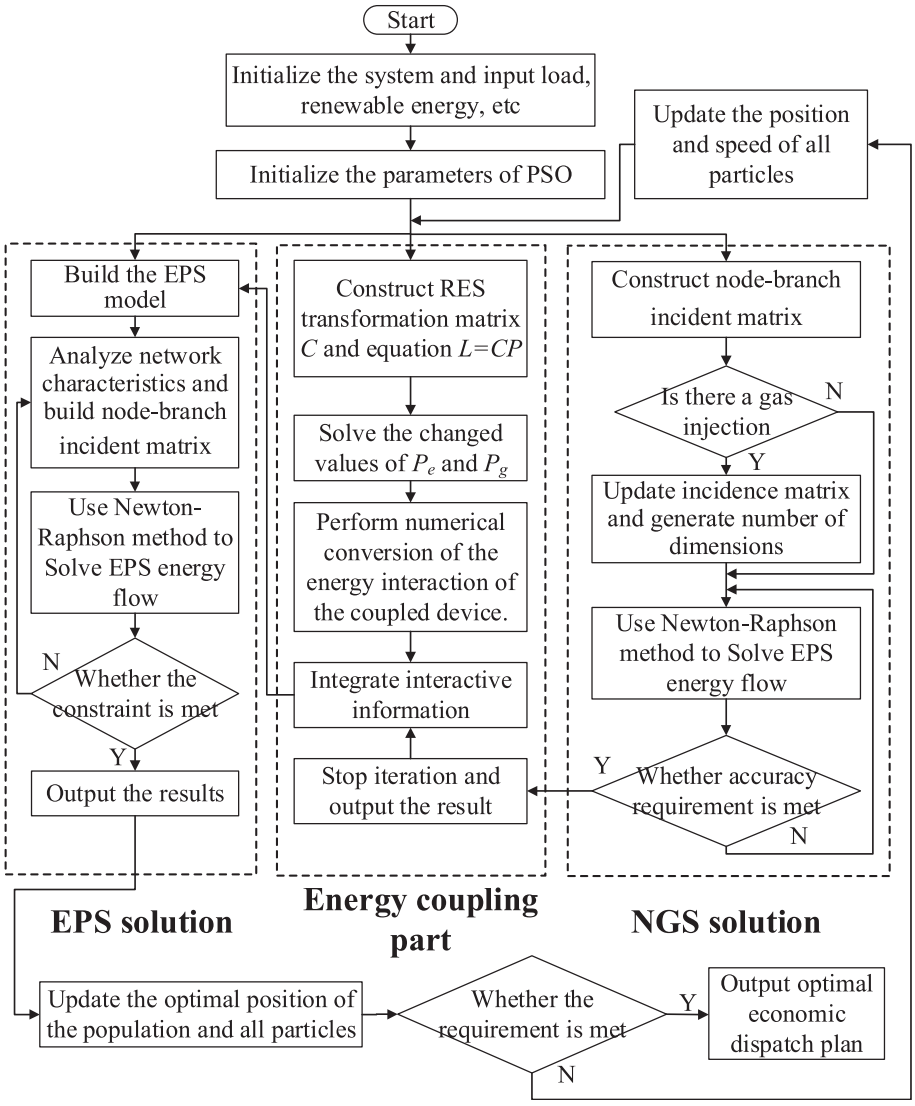

Fig. 2. Flow chart of steady state analysis of REGS.

Table 1 [25]. The setting of the case is shown in Table 2.

4.2. Operating cost and wind power consumption analysis

The operating costs of the RES and the wind power consumption rates in four scenarios are shown in Table 3 and Fig. 5, respectively.

It is clear that compared with Case 1, the economics of Case 2 improved significantly. The total cost of the coupling part in Case 2 decreased by 609.582$, which was 35.33% lower than that of Case 1. This was because the multienergy flow optimization was achieved by adjusting the distribution coefficient of the RES. Therefore, the total resource of the system was configured optimally and the economy was optimal. In Case 3, the operating cost was further reduced by the adjustment of the distributed gas injection point. The RES day-ahead total cost of energy in Case 3 was 38.75% and 5.3% lower than those of Cases 1 and 2, respectively. As shown in Table 3, the distributed gas injection point could help improve the economics of the RES operation. Furthermore, when the price of hydrogen or upgraded biogas decreased, the reduction in gas injection costs further reduced the total operating cost. Meanwhile, the temperament of the injected gas affected the operating cost. The RES day-ahead total cost of energy in Case 4 was reduced by 41.13%, 8.9%, and 3.87% compared with those of Cases 1, 2, and 3, respectively. When hydrogen was used as the temperament of the injected gas, the economics of the RES was better.

As shown in Fig. 5, the wind power consumption rates increased with the coordinated operation of the multienergy flow and the introduction of distributed gas injection points in Cases 2, 3, and 4. First, the RES operation improved the load level of the EPS and reduced the output power of CHP, thereby increasing the wind power consumption rate. Additionally, the distributed gas injection point effectively enhanced the gas pressure, resulting in more gas being input to the RES from the NGS. Therefore, the ability of the EPS in absorb wind power improved. Meanwhile, the increase in wind power consumption rate reduced the cost of wind curtailment, thereby increasing the economics of the RES.

4.3. Analysis of operating conditions of RES

4.3.1. Optimization of RES without gas injection

Fig. 6(a) shows the distribution coefficient of the RES for Case 2. Fig. 6(b) shows the RES input power of electricity. Fig. 6(c) shows the RES input power of natural gas and Fig. 6(d) shows the node pressure of the NGS.

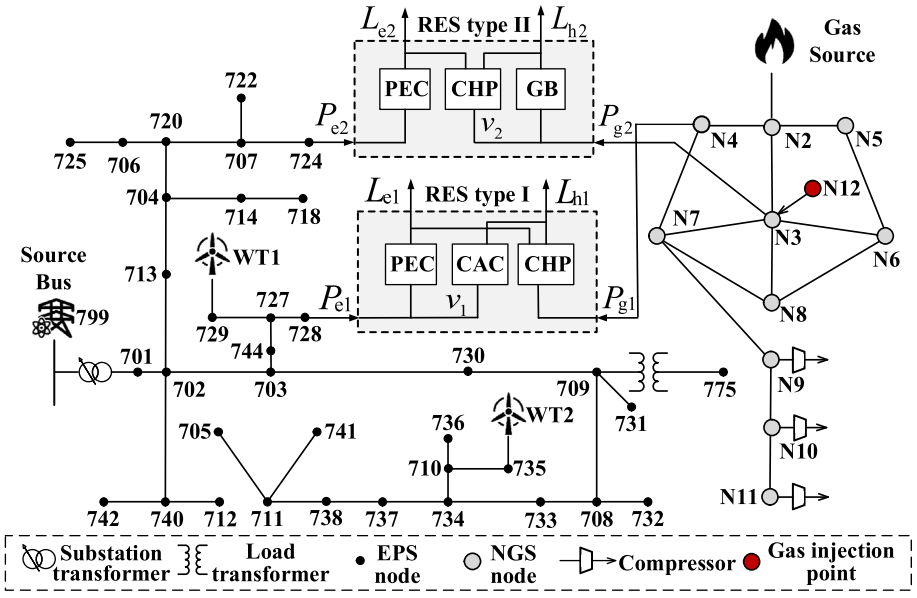

Fig. 3. REGS network structure.

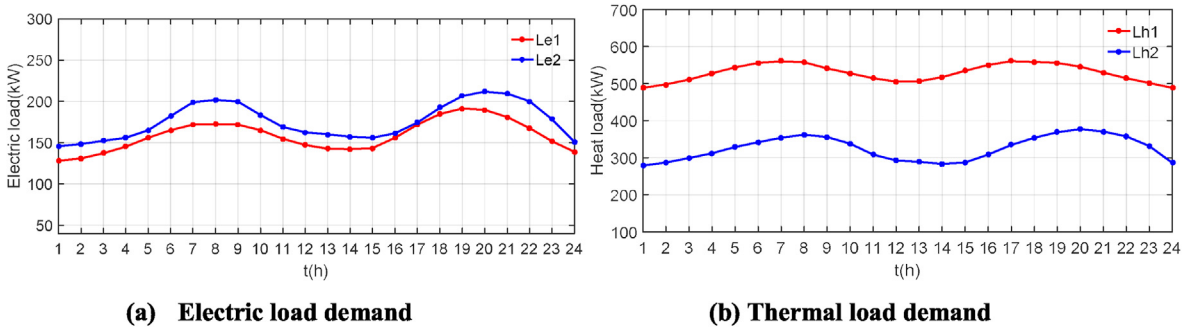

Fig. 4. The electric load and thermal load demand of RES.

Table 1
Energy prices.

Energy Price	Electricity ($/kWh)	Gas($/kWh)	Hydrogen ($/m^3)	Upgrade Biogas ($/m^3)
1:00–8:00	0.078	0.0425	0.075	0.068
9:00–21:00	0.1	0.0425	0.075	0.068
22:00–24:00	0.078	0.0425	0.075	0.068

Table 2
Setting of the case.

Case Setting	Case Description
Case 1	NGS which doesn't consider gas injection point, economic dispatch of RES decoupling energy system
Case 2	NGS which doesn't consider gas injection point, economic dispatch of RES coupled energy system
Case 3	NGS which considers the gas injection temperament as the injection point of upgrade biogas, and the RES economic dispatch of coupled operation
Case 4	NGS which considers the gas injection temperament as the injection point of hydrogen, and the RES economic dispatch of coupled operation

Table 3
Cost of four scenarios for daily operation.

Type	Cost of RES/$	Cost of abandoned wind power/$	Cost of gas injection/$	Total cost/$
Case 1	1725.492	1.808	0	1727.3
Case 2	1115.91	1.59	0	1117.5
Case 3	1056.69	1.36	243.42	1301.5
Case 4	1015.8	1.32	274.58	1291.7

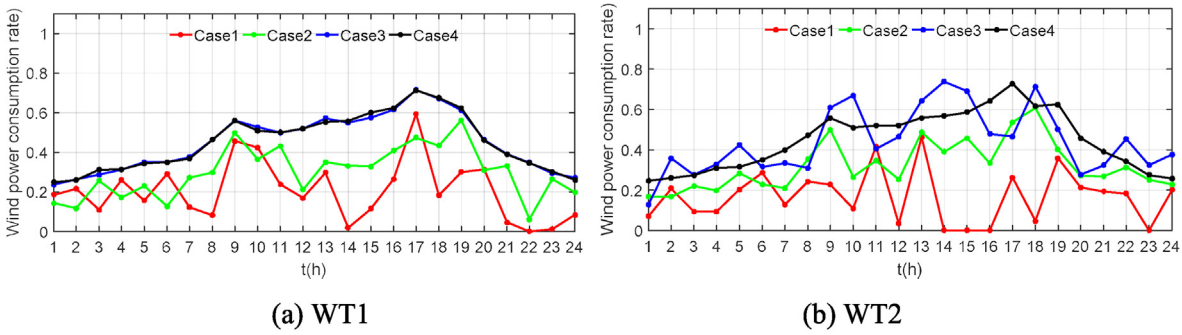

Fig. 5. The wind power consumption rate of WT1 and WT2.

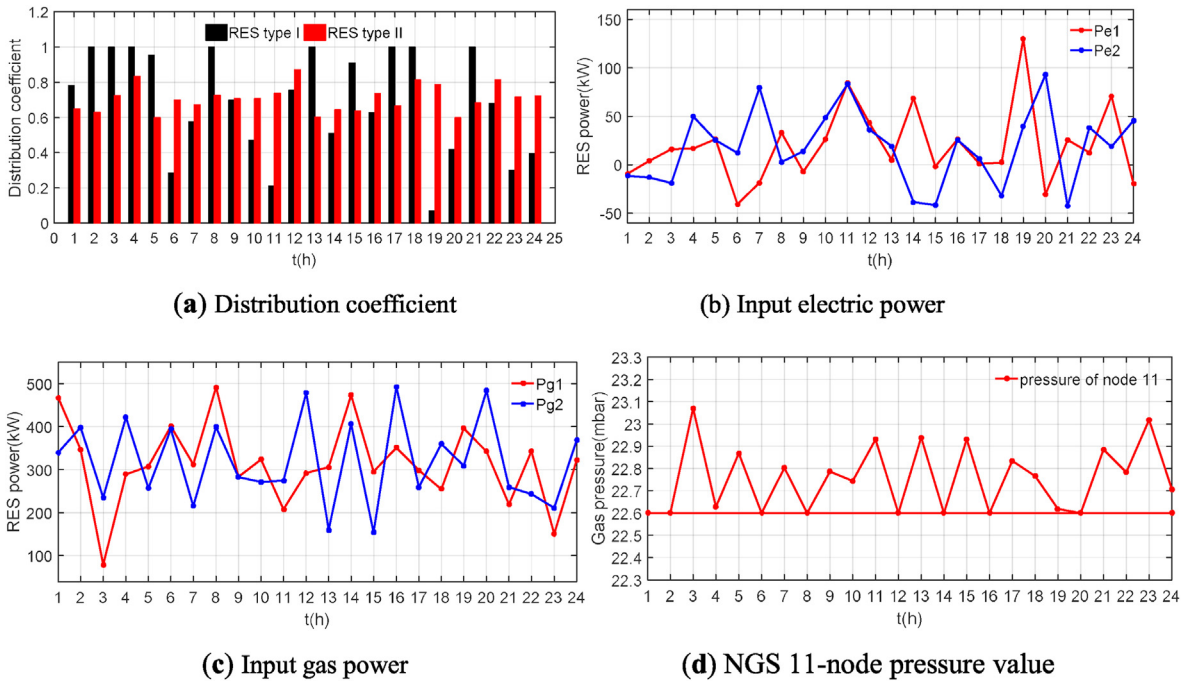

Fig. 6. Optimization results of RES without gas injection.

As shown in Fig. 4(a) and (b), the load demand of the RES presents two peaks and one valley. From 7:00 to 10:00, owing to the high electricity price, to reduce the economic cost, Type I RES primarily uses natural gas by CHP to satisfy the electric load demand. The specific details are as follows:

1) The natural gas power absorbed by the type I RES in Fig. 6(c) reached the peak. Furthermore, the absorbed electric power was low, as shown in Fig. 6(b) (by the red line in the figure).
2) The distribution coefficient $v1$ in Fig. 6(a) was the largest (shown in the black histogram), and the proportion of electricity load supplied by the consumed electric power was the lowest in the total electricity load.

The type I RES satisfied the heat load demand primarily by a CAC and CHP during the thermal load peak from 17:00 to 19:00. Because the heating efficiency of the CAC is much higher than that of CHP, the thermal demand in this stage is more likely to be satisfied by the CAC. It was observed that the absorbed power of natural gas reduced (see Fig. 6(c)), and the absorbed electric power exhibited an upward trend (see Fig. 6(b)).

As shown in Fig. 6(b) and (d), the type II RES satisfied the power load primarily by the PECs at the peak of electrical load from 20:00 to 22:00. This occurred because the input gas of the RES was limited owing to the limitation of the NGS operation. CHP could not satisfy the power load demand; therefore, the type II RES supplied the electric load by the PECs. During the optimal dispatch process, the voltage of the EPS nodes, the NGS node pressure, and the NGS pipeline flow were all within the reasonable range.

4.3.2. Optimization of RES with gas injection of upgraded biogas

For Case 3, the economic dispatch results of the NGS considering the gas injection point are shown in Fig. 7(a) and (b), 7(c), and 7(d). Two main effects on the NGS with gas injection were observed: the pressure level of the system and the pipeline flow of the system were affected. This affected the relationship between the NGS pressure level and the natural gas power absorbed by the RES.

Considering that the 11-th node in the NGS was at the end of the pipeline and supplied by a single pipeline, the load change affected the system pressure level the most. Therefore, the 11-th node was compared and optimized. As shown in Fig. 7, the injection of the upgraded biogas resulted in a significant improvement in the total

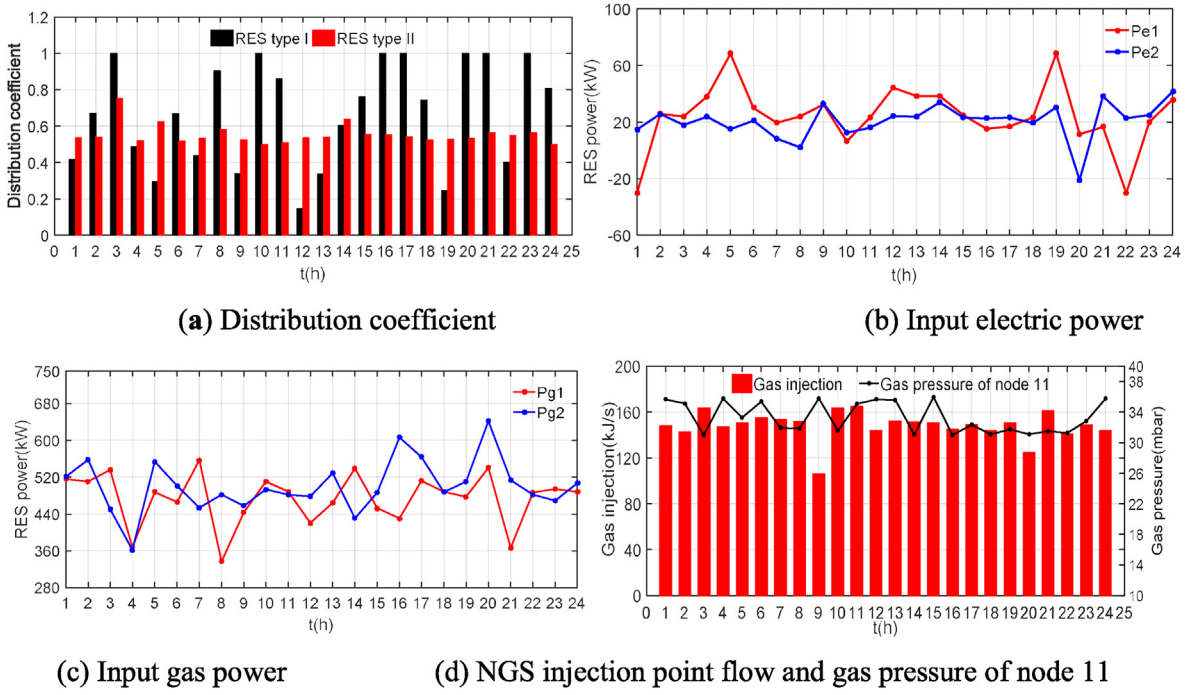

Fig. 7. Optimization results of RES with gas injection of upgrade biogas.

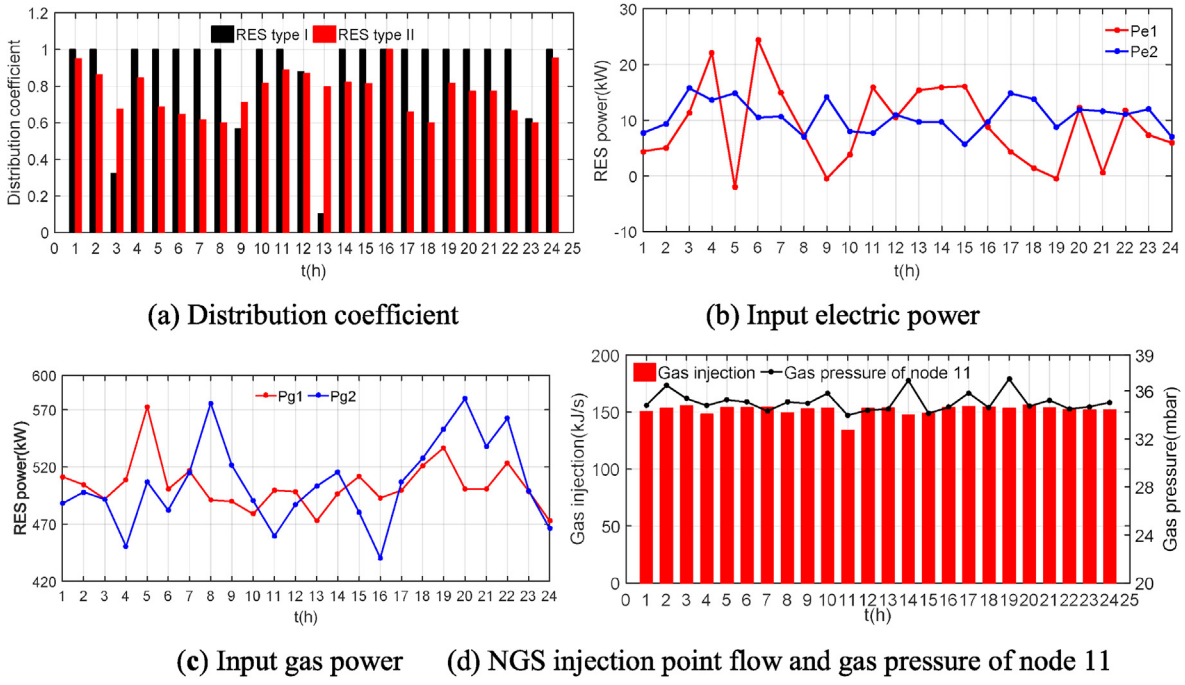

Fig. 8. Optimization results of RES with gas injection of hydrogen.

pressure level of the NGS. Under the same load, the pressure drop of the NGS in Case 3 was smaller; therefore, it could supply more load. This was because the upgraded biogas and natural gas have different specific gravities (SGs). The SG not only affects the energy released by the natural gas with different temperaments, but also affects the system pressure level. Specifically, the SG of the upgraded biogas gas was smaller than that of the natural gas; therefore, the system in Case 3 exhibited a lower pressure drop level.

The NGS pressure level improved by increasing the natural gas absorption power of the type II RES. Without considering the injection of upgraded biogas, the pressure at the 11-th node in Fig. 6(d) approached the lower boundary, which resulted in the limitation of the NGS output and the low natural gas input of the RES. By injecting the upgraded biogas, the NGS pressure level and load supply capacity of the RES increased, which increased the natural gas power absorbed by the RES. Compared with Case 2, as shown in Fig. 7(c) and (a), the power load of the type II RES was

primarily satisfied by CHP, which consumed natural gas at the peak of the electrical load from 20:00 to 22:00. As shown in Fig. 7(a), the distribution coefficient $v2$ of RES type II was at a higher level. At this time, the weight of the corresponding consumed natural gas increased.

Simultaneously, for the type I RES from 18:00–20:00, it was more inclined to supply heat load by CHP owing to the increase in the NGS load supply capacity. As shown in Fig. 7(c), the power of the natural gas absorbed by the type I RES improved, and the absorbed electric power decreased. Despite the high distribution coefficient $v1$, the amount of heat converted by the CAC was small.

4.3.3. Optimization of RES with gas injection of hydrogen

When hydrogen was used as the gas injection temperament, the economic dispatch results of the system are as shown in Fig. 8(a) and (b), 8(c), and 8(d).

The figures show that injecting hydrogen is more effective in improving the pressure distribution of the NGS. Using the 11th node in the NGS as an example, it was observed that the pressure improved. This occurred because the SG of the hydrogen was smaller than that of the upgraded biogas. In this case, the NCS pressure drop was smaller in Case 4 than that in Case 3. Compared with Fig. 7(d), the pressure value of the 11th node in Case 4 was larger, and the change between different times was more gradual. However, the GCV of hydrogen was extremely small, implying that more hydrogen must be burned to satisfy the same energy demand compared with the upgraded biogas. Considering that the gas price was lower than the electricity price, in an economical dispatch, the gas power absorbed by the RES increased and the electric power absorbed by the RES decreased, which indirectly increased the voltage support effect of the EPS.

From 19:00 to 21:00, owing to the high electricity price and the increase in the gas power absorbed by the RES, the type II RES used primarily natural gas by CHP to satisfy the electric load demand to reduce the economic cost. The specific details are as follows:

1) The natural gas power absorbed by the type II RES in Fig. 8(c) reached the peak.
2) The distribution coefficient $v2$ of RES type II in Fig. 8(a) was at a high level, and the proportion of electricity load supplied by the gas power increased the total electricity load.

The Type I RES satisfied the electricity load demand primarily by CHP from 18:00 to 20:00 because of the increase in the natural gas supply capacity and the high electricity price. The main reasons are as follows:

1) The power of the natural gas absorbed by the type I RES in Fig. 8(c) was high.
2) In Fig. 8(a), the distribution coefficient $v1$ reached the peak. At this time, the proportion of electricity load supplied by natural gas was 100%.

4.3.4. Analysis of NGS sensitivity

The 24 h operation of the NGS was selected to analyze the system's natural-gas-pressure–load sensitivity results. The results facilitated in the selection of nodes that were sensitive to the system pressure and in the implementation of the load regulation. The node-pressure–load-sensitivity matrix S of the NGS is shown in Table 4.

The element $\boldsymbol{s}_{x,y}(x,y = 2,3,\cdots,11)$represents the effect of node x's load change on the pressure of node y, where Node 1 is the gas source point and its pressure is constant. The bold red element in each row of S represents the maximum value of the row. It implies that node x's load change exerts the greatest effect on the pressure generated by node y. As shown from the sensitivity matrix, the large element of the matrix value appears in the lower right corner box. The 11th node corresponds to the maximum value. This was because nodes 9–11 were at the end of the pipeline and supplied by a single pipeline. The load change exerted the greatest effect on the system pressure, which was consistent with the actual situation of the network. The load regulation at this point was the most effective in improving the pressure level of the NGS.

In summary, the introduction of NGS distributed gas injection points improved the pressure drop level of the NGS and further improved the economics of the system operation. Meanwhile, it contributed positively to the stability improvement of the RIES.

5. Conclusion

In the context of RIESs, EPS, NGS, and RES models were constructed in this study, and a comprehensive REGS model that considered gas injection was proposed. In the analysis of the REGS, a discrete solution method was used to calculate the multienergy flow. In the simulation of a typical REGS case, the optimization objectives and operational constraints in four different scenarios were considered. It was discovered from the economic dispatching results that the introduction of NGS distributed gas injection improved the pressure drop level of the NGS and the economics of the system operation. Meanwhile, it effectively improved the wind power consumption rate of the EPS, which contributed positively to the stability improvement of the RIES. Among them, the RES economy was optimal under the scheme of hydrogen gas injection, and the wind power consumption rate was the highest. With the development of energy conversion technologies such as CHP and P2G and the integration of renewable energy technologies, coupling between multiple energies is strengthened. The

Table 4
Node pressure-load sensitivity matrix of NGS.

		Pressure change (node)									
		Node2	Node 3	Node 4	Node 5	Node 6	Node 7	Node 8	Node 9	Node 10	Node 11
load change (node)	Node 2	0.012	0.012	0.012	0.012	0.012	0.012	0.012	0.012	**0.012**	0.012
	Node 3	0.015	**0.056**	0.032	0.039	0.047	0.047	0.049	0.047	0.047	0.047
	Node 4	0.016	0.034	**0.122**	0.031	0.036	0.058	0.041	0.058	0.058	0.058
	Node 5	0.017	0.045	0.033	**0.111**	0.076	0.048	0.060	0.048	0.048	0.048
	Node 6	0.018	0.054	0.039	0.077	**0.096**	0.059	0.076	0.059	0.059	0.059
	Node 7	0.017	0.055	0.062	0.048	0.058	0.103	0.069	0.103	**0.103**	0.103
	Node 8	0.018	0.058	0.045	0.062	0.076	0.071	**0.099**	0.071	0.071	0.071
	Node 9	0.021	0.067	0.076	0.059	0.072	0.127	0.085	0.293	**0.293**	0.293
	Node 10	0.023	0.073	0.082	0.064	0.078	0.137	0.092	0.318	**0.405**	0.405
	Node 11	0.024	0.074	0.083	0.065	0.079	0.139	0.094	0.322	0.411	**0.446**

comprehensive model proposed herein provides a basis for the further development of IESs. In the future, two aspects should be further investigated: the synergistic optimization of multienergy systems and the multiple gas injection points of NGSs.

Declaration of competing interests

The authors declare that they have no known competing financial interests or personal relationships that could have appeared to influence the work reported in this paper.

CRediT authorship contribution statement

Gui-Xiong He: Conceptualization, Methodology, Formal analysis, Data curation, Writing - original draft. **Hua-guang Yan:** Writing - review & editing, Investigation. **Lei Chen:** Writing - review & editing, Validation. **Wen-Quan Tao:** Writing - review & editing, Supervision.

Acknowledgments

This work is supported by the State Grid Corporation of China Project: “Intelligent energy network optimization, simulation and application of the park ‘Internet +’ based on the source and load characteristics information (SGTYHT/16-JS-198).”

References

[1] Jia HJ, Wang D, Xu XD, et al. Research on some key problems related to integrated energy systems. Autom Electr Power Syst 2015;39(7):198–207.
[2] Wang Weiliang, Wang Dan, Jia Hongjie, et al. Review of steady-state analysis of typical regional integrated energy system under the background of energy internet. Proceedings of the Csee 2016;36(12):3292–305.
[3] Xiaodan Y, Xiandong X, Shuoyi C, et al. A brief review to integrated energy system and energy internet. Trans China Electrotech Soc 2016;31(1):1–13.
[4] Guan L, Chen P, Tang ZS, et al. Integrated energy station design considering cold and heat storage. Power Syst Technol 2016;40(10):2934–41.
[5] Li Q, An S, Gedra TW. Solving natural gas loadflow problems using electric loadflow techniques. Proc of the North American Power Symposium 2003: 1–7.
[6] Geidl M, Andersson G. A modeling and optimization approach for multiple energy carrier power flow. Power Tech 2005:1–7. IEEE Russia. IEEE. 2005.
[7] Shahidehpour M, Fu Y, Wiedman T. Impact of natural gas infrastructure on electric power systems. Proc IEEE 2005;93(5):1042–56.
[8] Abeysekera M, Wu J, Jenkins N, et al. Steady state analysis of gas networks with distributed injection of alternative gas. Appl Energy 2016;164: 991–1002.
[9] Trifonov Teodor Ognyanov. Coordination of battery energy storage and power-to-gas in distribution systems. Protection and Control of Modern Power Systems 2017;2(1):38.
[10] Wang W, Wang D, Jia HJ, et al. A decomposed solution of multi-energy flow in regional integrated energy systems considering operational constraints. Energy Procedia 2017;105:2335–431.
[11] Ma Z, Chen H, Chai Y. Analysis of voltage stability uncertainty using stochastic response surface method related to wind farm correlation. Protection and Control of Modern Power Systems 2017;2(1):1–9.
[12] Wang Weiliang, Wang Dan, Jia Hongjie, et al. Steady state analysis of electricity-gas regional integrated energy system with consideration of NGS network status. Proceedings of the Csee 2017;37(5):1293–304.
[13] Osiadacz AJ. Simulation and analysis of gas networks. E. & F.N. Spon; 1987.
[14] Chen Sheng, Wei Zhinong, Sun Guoqiang, et al. Probabilistic energy flow analysis in integrated electricity and natural-gas energy systems. Proceedings of the Csee 2015;35(24):6331–40.
[15] Zhang Yibin. Study on the methods for analyzing combined gas and electricity networks. Beijing: China Electric Power Research Institute; 2005.
[16] Liu L, Wang D, Jia HJ, et al. Integrated modeling and energy optimization analysis of generalized multi-source energy storage system. Electric Power Construction 2017;38(12):2–11.
[17] Liu X, Jenkins N, Wu J, et al. Combined analysis of electricity and heat networks. Energy Procedia 2014;61:155–9.
[18] Qadrdan M, Abeysekera M, Chaudry M, et al. Role of power-to-gas in an integrated gas and electricity system in great britain. Int J Hydrogen Energy 2015;40(17):5763–75.
[19] Schiebahn S, Grube T, Robinius M, et al. Power to gas: technological overview, systems analysis and economic assessment for a case study in Germany. Int J Hydrogen Energy 2015;40(12):4285–94.
[20] Civan F. SPE gas technology symposium. In: Review of methods for measurement of natural gas specific gravity. Dallas, USA: Society of Petroleum Engineers; 1989.
[21] XianDong Xv. Modelling, simulation, and energy management Research for electricity, gas, and heat based micro energy system. Tianjin: Tianjin University; 2014.
[22] Liang Xie. Research on the algorithms and applications of optimal power flow based on interior point theory. Shanghai: Shanghai Jiao Tong University; 2011.
[23] Lin W, Jin X, Mu Y, et al. A two-stage multi-objective scheduling method for integrated community energy system. Appl Energy 2018;216:428–41.
[24] Xu X, Jin X, Jia H, et al. Hierarchical management for integrated community energy systems. Appl Energy 2015;160:231–43.
[25] Wang Weiliang, Wang Dan, Jia Hongjie, et al. Performance evaluation of a hydrogen-based clean energy hub with electrolyzers as a self-regulating demand response management mechanism. Energies 2017;10:1–23.